

Self-Condensation of $[\text{Mo}^{\text{V}}_2\text{O}_2\text{S}_2]^{2+}$ with Phosphate or Arsenate Ions by Acid–Base Processes in Aqueous Solution: Syntheses, Crystal Structures, and Reactivity of $[(\text{HXO}_4)_4\text{Mo}_6\text{S}_6\text{O}_6(\text{OH})_3]^{5-}$, $\text{X} = \text{P}, \text{As}$

Emmanuel Cadot, Anne Dolbecq, Bernadette Salignac, and Francis Sécheresse*

Abstract: The self-condensation of dithiocations $[\text{Mo}_2\text{S}_2\text{O}_2]^{2+}$ in aqueous solution in the presence of arsenate or phosphate ions as assembling groups led at pH 4–5 to hexanuclear $[\text{H}_7\text{X}_4\text{Mo}_6\text{S}_6\text{O}_{25}]^{5-}$ heteropolyoxothio anions **1** ($\text{X} = \text{P}$) and **2** ($\text{X} = \text{As}$). Both **1** and **2** were isolated in the solid state in good yield as mixed cesium–sodium salts and were characterized unambiguously by elemental analysis, IR and ^{31}P NMR spectroscopy, and single-crystal X-ray structural analysis. $\text{Rb}_4\text{Na}_{1.75}\text{Cl}_{0.75}[\text{H}_7\text{P}_4\text{Mo}_6\text{S}_6\text{O}_{25}] \cdot 8\text{H}_2\text{O}$ (**1b**) crystallizes in the rhombohedral space group $R\bar{3}$ ($a = 13.352(3)$, $b = 13.352(3)$, $c = 39.708(10)$ Å) and $\text{Rb}_{3.5}\text{Na}_{1.5}[\text{H}_7\text{As}_4\text{Mo}_6\text{S}_6\text{O}_{25}] \cdot 11\text{H}_2\text{O}$ (**2b**) in the triclinic $P\bar{1}$ space group ($a =$

$12.967(1)$, $b = 13.271(1)$, $c = 15.870(1)$ Å, $\alpha = 101.11(1)^\circ$, $\beta = 91.81(1)^\circ$, $\gamma = 115.94(1)^\circ$). The anions in **1b** and **2b** exhibit similar molecular structures, which consist of three $\{\text{Mo}_2\text{O}_2\text{S}_2\}$ units surrounding a single central XO_4 group and mutually connected by three hydroxo bridges and three peripheral phosphate or arsenate groups. There is an interesting possibility of substituting the peripheral XO_4 groups. A variable-temperature ^{31}P NMR study of **1** in solution revealed a dynamic exchange

Keywords: molybdenum • NMR spectroscopy • polyoxometalates • solid-state structure • sulfur

between peripheral phosphate groups and uncoordinated phosphate ions. ^{31}P NMR also gave evidence of the successive replacement of arsenate by phosphate groups in **2**. The apparent exchange constants that were calculated were in agreement with a nearly pure statistical exchange between arsenate and phosphate groups. The substitution of the phosphate by acetate ligands in **1** was also examined. ^{31}P NMR spectra agreed with the successive formation of the mono-, di- and triacetato complexes. The very good agreement between the calculated and experimental distribution of substituted compounds confirmed the ^{31}P NMR assignments and the proposed exchange scheme.

Introduction

Introduction of sulfur into the structure of polyoxometalates (POMs) is expected to modify both the electronic properties and the reactivity of these large species, but the direct sulfurization of the POM generally results in the reduction of metal atoms, together with the breakdown of the M–O skeleton; so far, only low-nuclearity thiometalates have been obtained in this way.^[1] To prevent the degradation of the POM, we first developed a simple and convenient method consisting of the stereospecific addition of the preformed $[\text{Mo}^{\text{V}}_2\text{S}_2\text{O}_2]^{2+}$ thio fragment to the divacant γ - $[\text{SiW}_{10}\text{O}_{36}]^{8-}$ and γ - $[\text{PW}_{10}\text{O}_{36}]^{7-}$ ions.^[2] Then we extended this protocol to the α - $[\text{PW}_{11}\text{O}_{39}]^{7-}$ and α - $[\text{PW}_9\text{O}_{34}]^{9-}$ polyvacant Keggin precursors to prepare sandwich-type species.^[3] All the com-

pounds obtained thus have a limited sulfur content imposed by the number of sulfur atoms present in the thio precursor. For this reason we have used a new synthetic route based on the self-condensation of the $[\text{Mo}_2\text{S}_2\text{O}_2]^{2+}$ building unit upon addition of a base. The first example we reported was the preparation and characterization of the cyclic neutral wheel $[\text{Mo}_{12}\text{S}_{12}\text{O}_{12}(\text{OH})_{12}(\text{H}_2\text{O})_6]$, obtained by direct addition of a solution of potassium hydroxide to a solution of $[\text{Mo}_2\text{S}_2\text{O}_2]^{2+}$.^[4] This product can be described as a molecular ring with a cavity about 11 Å in diameter, resulting from the cyclic condensation of six $\{\text{Mo}_2\text{S}_2\text{O}_2\}$ units with 12 hydroxo groups. In the presence of molybdate ions acting as a template, the condensation of $[\text{Mo}_2\text{S}_2\text{O}_2]^{2+}$ leads to the octameric ring $\{\text{Mo}_8\text{S}_8\text{O}_8(\text{OH})_8\}$ encapsulating a Mo^{VI} octahedron.^[5] We have now carried out the polycondensation (based on the same idea) of the $[\text{Mo}_2\text{S}_2\text{O}_2]^{2+}$ precursor in the presence of phosphate or arsenate ions as assembling groups. The thiomolybdophosphate system is expected to have a very abundant and diverse membership, comparable with the related oxomolybdophosphates, and to include discrete species, one-dimensional (1D) polymers, two-dimensional (2D)

[a] F. Sécheresse, E. Cadot, A. Dolbecq, B. Salignac
Institut Lavoisier, IREM, UMR C0173, Université de Versailles
Saint-Quentin
45 Avenue des Etats-Unis, F-78035 Versailles (France)
Fax: (+33) 1-39-25-43-81
E-mail: secheres@chimie.uvsq.fr

layered materials and three-dimensional (3D) solids.^[6] Most of these solids are generally obtained through high-temperature processes or hydrothermal syntheses and contain anionic P–M–P frameworks based on the $\{\text{Mo}_2\text{O}_4\}$ fragment and PO_4 tetrahedra, which occlude cations serving as 3D-structure directing agents. So far, only a few compounds illustrating the association of $[\text{Mo}_2\text{S}_2\text{O}_2]^{2+}$ with assembling groups are described in the literature,^[7] and in none of them are there direct connections between the $[\text{Mo}_2\text{S}_2\text{O}_2]^{2+}$ units. For example, the reaction between MoS_4^{2-} and As_4S_4 , under mild conditions, is reported to give molecular compounds containing a $[\text{Mo}_2\text{S}_2\text{O}_2]^{2+}$ core strapped by $[\text{As}^{\text{V}}_4\text{S}_{12}]^{4-}$ and $[\text{As}^{\text{III}}_2\text{S}_3]^{4-}$ chelates.^[8] More recently, 1D polymeric $(\text{NMe}_4)_2[\text{Mo}_2\text{O}_2\text{As}_2\text{S}_7]$ was obtained in hydrothermal conditions from mixtures containing MoO_3 and $\text{K}_3[\text{AsS}_3]$,^[9] the structure being described as the 1D arrangement of $\{\text{Mo}_2\text{S}_2\text{O}_2\}$ fragments linked by $\{\text{As}_2\text{S}_3\}$ units. In this example, hydrothermal conditions are required to promote the reduction of the starting MoO_3 to form the Mo^{V} dinuclear fragment. As hydrothermal conditions can display some drawbacks, such as limitations on characterizations in situ,^[10] we carried out the syntheses in solution, under mild conditions, starting from the early-reduced Mo^{V} precursor $[\text{Mo}_2\text{S}_2\text{O}_2]^{2+}$. The syntheses and complete structural characterizations of $[\text{H}_7\text{X}_4\text{Mo}_6\text{S}_6\text{O}_{25}]^{5-}$

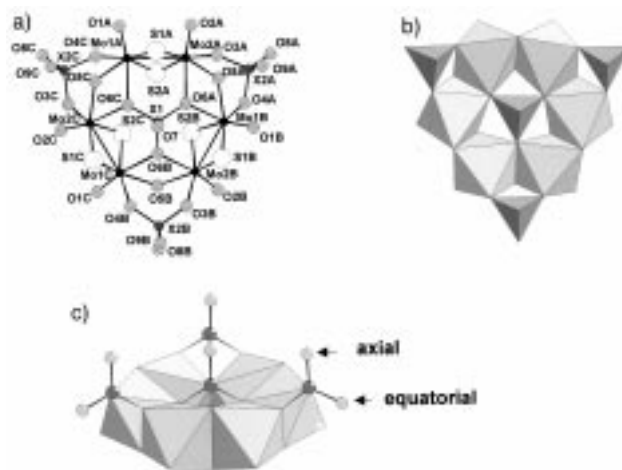
ions, X = P (**1**) or As (**2**), are reported here, together with a study of their chemical reactivity.

Results and Discussion

Preparation of $[\text{H}_7\text{X}_4\text{Mo}_6\text{S}_6\text{O}_{25}]^{5-}$ (1**, **2**):** The synthesis of the anionic clusters is quite straightforward starting from an aqueous solution of $[\text{Mo}_2\text{S}_2\text{O}_2]^{2+}$ prepared by hydrolysis of $[\text{Mo}_{12}\text{S}_{12}\text{O}_{12}(\text{OH})_{12}(\text{H}_2\text{O})_6]$ in 4 M HCl.^[4] The anions **1** and **2** were isolated in good yield in the solid state as cesium salts **1a** and **2a**. Both anions **1** and **2** are stable only in more highly concentrated phosphate or arsenate solutions ($>0.3\text{M}$). The poor stability of these anions in solution is related to the lability of the peripheral XO_4 groups as revealed by ^{31}P NMR studies (see below). With a lower phosphate concentration, another polymeric anion was obtained, $[(\text{HPO}_4)_2\text{Mo}_{12}\text{S}_{12}\text{O}_{12}(\text{OH})_{12}(\text{H}_2\text{O})_2]^{4-}$,^[11] described as an elliptical ring derived structurally from the cyclic precursor $[\text{Mo}_{12}\text{S}_{12}\text{O}_{12}(\text{OH})_{12}(\text{H}_2\text{O})_6]$ ^[4] by the replacement of four inner water molecules by two phosphate ions.

Molecular structure of $\text{Na}_{1.75}\text{Rb}_4\text{Cl}_{0.75}[\text{H}_7\text{P}_4\text{Mo}_6\text{S}_6\text{O}_{25}] \cdot 8\text{H}_2\text{O}$ (1b**):** The molecular structure of anion **1b** (Figure 1) is similar to that of the analogous oxo system, widely described in the

Abstract in French: La polycondensation de l'entité dithiocationique $[\text{Mo}_2\text{S}_2\text{O}_2]^{2+}$ en présence d'arsénate ou de phosphate comme élément assembleur conduit en milieu aqueux vers pH 4–5 aux polyanions hexanucléaires $[\text{H}_7\text{X}_4\text{Mo}_6\text{S}_6\text{O}_{25}]^{5-}$ notés **1** pour X = P et **2** pour X = As. Les deux anions sont isolés à l'état solide avec un bon rendement sous la forme de sels mixtes de césium et de sodium et ont été caractérisés sans ambiguïté par leur analyse élémentaire, les spectroscopies IR et RMN de ^{31}P et par diffraction des rayons X sur monocristal. $\text{Rb}_4\text{Na}_{1.75}\text{Cl}_{0.75}[\text{H}_7\text{P}_4\text{Mo}_6\text{S}_6\text{O}_{25}] \cdot 8\text{H}_2\text{O}$ (**1b**) cristallise dans le groupe d'espace rhomboédrique $R\bar{3}$ ($a = 13.352(3)\text{ \AA}$, $b = 13.352(3)\text{ \AA}$, $c = 39.708(10)\text{ \AA}$) et $\text{Rb}_{3.5}\text{Na}_{1.5}[\text{H}_7\text{As}_4\text{Mo}_6\text{S}_6\text{O}_{25}] \cdot 11\text{H}_2\text{O}$ (**2b**) cristallise dans le groupe d'espace triclinique $P\bar{1}$ ($a = 12.967(1)$, $b = 13.271(1)$, $c = 15.870(1)\text{ \AA}$, $\alpha = 101.11(1)^\circ$, $\beta = 91.81(1)^\circ$, $\gamma = 115.94(1)^\circ$). Les anions **1** et **2** présentent la même structure moléculaire : trois unités $\{\text{Mo}_2\text{S}_2\text{O}_2\}$ sont connectées deux à deux autour d'un tétraèdre central XO_4 , par un pont hydroxo et par un phosphate ou arsenate périphérique. Ces composés présentent une réactivité particulière basée sur la substitution des ligands XO_4 périphériques. Une étude par RMN à température variable sur des solutions de **1** et de phosphate a montré qu'un échange dynamique existe entre les phosphates périphériques et les phosphates libres. D'autre part, la RMN de ^{31}P a montré que les arsenates périphériques de **2** peuvent s'échanger avec des phosphates. Les constantes apparentes correspondant aux équilibres successifs ont été calculées et montrent que la distribution des groupes XO_4 périphériques est quasi-statistique. La substitution des phosphates périphériques dans **1** par l'acétate a aussi été étudiée, illustrant la formation successive des dérivés mono, di et tri acétato. L'excellent accord entre la distribution calculée et expérimentale confirme les attributions des signaux RMN et la validité du processus d'échange.



arrangements based on dinuclear $\{\text{Mo}_2\text{O}_2\text{E}_2\}$ ($\text{E} = \text{O}, \text{S}$) units.^[4, 5, 12–16] The connections between each building unit are edge-sharing (Figure 1 b) and not face-sharing as observed in $[\text{Mo}_{12}\text{S}_{12}\text{O}_{12}(\text{OH})_{12}(\text{H}_2\text{O})_6]^{4-}$,^[4] $[\text{Mo}_9\text{S}_8\text{O}_{12}(\text{OH})_8(\text{H}_2\text{O})_2]^{2-}$,^[5] and $[\text{Mo}_8\text{S}_8\text{O}_8(\text{OH})_8(\text{C}_2\text{O}_4)]^{2-}$.^[16] The resulting hexanuclear ring encapsulates a central phosphate group and is stabilized by three peripheral phosphate ligands. The four PO_4 groups lie on the same side of the mean plane defined by the six molybdenum atoms (Figure 1 c). Each peripheral phosphate group exhibits a long P–O separation (1.583(8) Å), characteristic of a protonated P–OH bond, and a shorter one (1.498(8) Å), attributed to a P=O bond. The central phosphate group is assumed to be protonated so that the polyanion has an overall charge of -5 , in agreement with the presence of 5.75 alkali metal cations and 0.75 chloride anions, as determined by elemental analysis. The corresponding P1–O7 distance (1.508(10) Å) in the central phosphate group is quite short for a P–OH bond. The locations of the protons are in accordance with those observed for the related arsenato compound **2b** (see below), which clearly displays a central X–OH bond. In summary, of the seven hydrogen atoms in the $[\text{H}_7\text{P}_4\text{Mo}_6\text{S}_6\text{O}_{25}]^{5-}$ ion, three are located on the Mo–O μ -oxo bridges, three on the peripheral PO_4 groups and one on the central PO_4 group. On the basis of the structural analysis, the detailed chemical formula of the anionic cluster in **1b** is thus $[(\text{HPO}_4)_4\text{Mo}_6\text{S}_6\text{O}_6(\text{OH})_3]^{5-}$. The location of three hydrogen atoms on the Mo–O μ -oxo bridges is similar to that usually observed for the comparable exclusively oxo compounds.^[13–15] However, depending on the synthesis conditions and the nature of the counterions, the number and distribution of the protons among the four phosphato groups have been shown to vary.^[14] In **1b**, the P=O bonds (P2–O9) of the peripheral PO_4 groups and the P–OH bond (P1–O7) of the central PO_4 group are almost perpendicular to the Mo plane (axial positions), while the protonated oxygen atoms (O8) occupy the corresponding equatorial positions (Figure 1 c).

Three-dimensional structure of 1b: Two rubidium atoms and one Na^+ ion (Na1) were located unambiguously. Na2 was found to be disordered and was assigned, after refinement, an occupancy factor of $5/12$. The chlorine atom Cl1 was placed at the origin of the cell (the center of the octahedron defined by six equivalent Rb1 atoms). An additional chlorine atom (Cl2) was located in a general position, with an occupancy factor of $1/2$, in agreement with the chemical analysis. The Rb1–Cl1 distance (3.257(1) Å) in the ClRb_6 octahedra is quite similar to that reported for the close-packed arrangement of the ionic solid RbCl (3.28 Å). The 3D structure of **1b** can be viewed as that of a multilayered solid (Figure 2). The Rb^+ ions ensure the connections between $[\text{H}_7\text{P}_4\text{Mo}_6\text{S}_6\text{O}_{25}]^{5-}$ ions forming planes parallel to the (001) plane. Each Rb^+ cation is directly linked to $[(\text{HPO}_4)_4\text{Mo}_6\text{S}_6\text{O}_6(\text{OH})_3]^{5-}$ polyanions by oxygen or sulfur atoms. The layers are interleaved alternately by sodium cations and Cl1 anions.

Structure of $\text{Rb}_{3.5}\text{Na}_{1.5}[\text{H}_7\text{As}_4\text{Mo}_6\text{S}_6\text{O}_{25}] \cdot 13\text{H}_2\text{O}$ (2b): The overall molecular arrangement of **2b** is quite similar to that of **1b**. The three peripheral arsenate groups exhibit short (1.654(8)–1.675(8) Å) As–O distances corresponding to

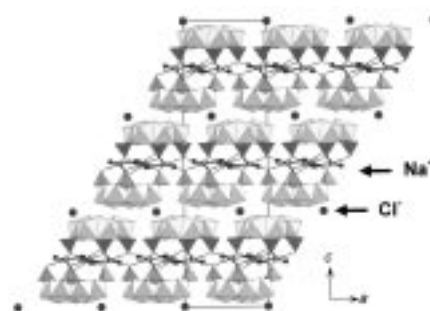


Figure 2. Polyhedral view of the $[(\text{HPO}_4)_4\text{Mo}_6\text{S}_6\text{O}_6(\text{OH})_3]^{5-}$ ions in **1b** showing the connection of anionic units by Na^+ ions and the multilayered structure.

As=O bonds, and longer (1.728(8)–1.734(8) Å) ones, attributed to As–OH bonds. The quite long As1–O7 distance (1.720(7) Å) between the central arsenate group and the terminal oxygen atom indicates that this oxygen atom is protonated. However, the proton distributions of **1b** and **2b** appear to differ slightly. In **2b**, the three As–OH bonds are perpendicular to the Mo plane (axial positions), while the oxygen atoms of the As=O bonds (1.654(8)–1.675(8) Å) occupy the equatorial positions. Each $[\text{H}_7\text{As}_4\text{Mo}_6\text{S}_6\text{O}_{25}]^{5-}$ unit is connected to three others, through strong As=O \cdots H–O–As hydrogen bonds involving the peripheral AsO_4 groups (Figure 3).

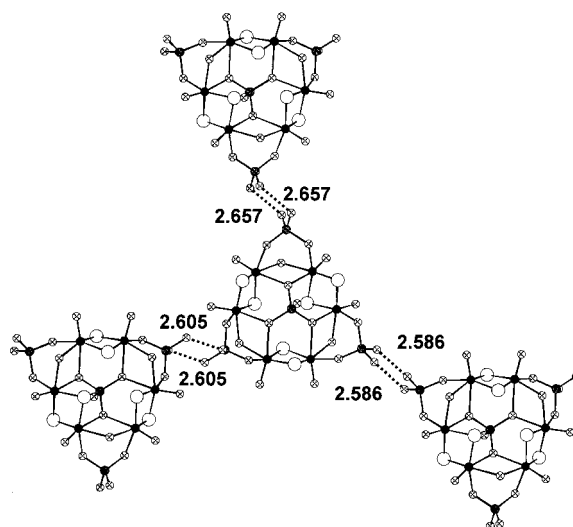


Figure 3. Hydrogen bonding pattern and the As=O \cdots HO–As distances [Å] within the anionic layers in the structure of **2b**.

^{31}P NMR characterization of $[\text{H}_7\text{P}_4\text{Mo}_6\text{S}_6\text{O}_{25}]^{5-}$ (1): ^{31}P NMR measurements have shown that the formation of the phosphato anion is rapid. A typical spectrum (Figure 4) of a synthesis solution at pH 4.80, recorded at 296 K, consists of three lines: the resonance at $\delta = +1.10$ is attributed to uncoordinated phosphate and the two remaining lines to the two nonequivalent types of phosphate present in the polyanion of C_{3v} symmetry. From intensity considerations, the $\delta = +2.70$ line (δ_p) is attributed to the three equivalent peripheral phosphate groups, while the $\delta = +4.40$ line (δ_c) is assigned to the single central phosphate group. Variable-temperature

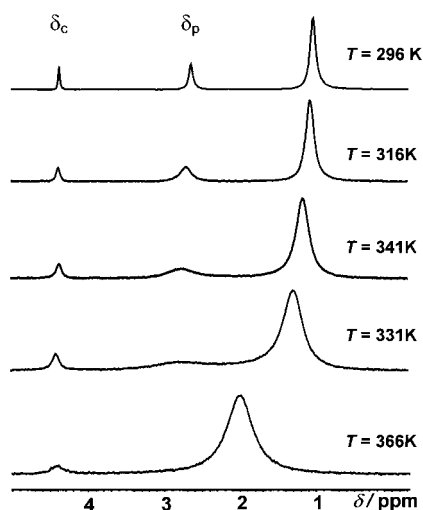


Figure 4. Variable-temperature ^{31}P NMR spectra of the synthesis solution for $[(\text{HPO}_4)_4\text{Mo}_6\text{S}_6\text{O}_6(\text{OH})_3]^{5-}$ (**1**).

^{31}P NMR experiments on the synthesis solution at pH 4.8 (Figure 4) showed that the two resonances attributed to uncoordinated phosphate ions and to peripheral PO_4 groups are the most sensitive to an increase of temperature. Both lines broaden in the 296–366 K range and then overlap. At 366 K the spectrum consists of two resonances: the line characteristic of the central phosphate group near $\delta = +4.0$ and a broad line at $\delta = +2.0$ corresponding to a rapid exchange between peripheral and uncoordinated phosphate groups. Both chemical shifts appear to be pH-dependent (Figure 5). An increase in pH from 2 to 6 results in deshielding of the central phosphorus nucleus, while a shielding effect is observed for the peripheral phosphate groups.

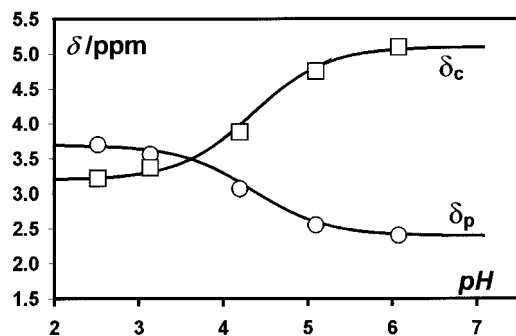


Figure 5. pH dependence of the chemical shifts of the central (δ_c) and peripheral (δ_p) phosphate lines in **1b**.

The variation of δ_c with pH is that expected for phosphates directly involved in a proton exchange. A pK_a of 4.35 for the corresponding equilibrium is obtained from the variation of δ_c and δ_p with pH (Figure 5). The opposite shift observed for the δ_p resonance was attributed to the variation of the charge on the polyanion due to the loss of the proton on the central phosphate group. Such behavior was reported previously for the trisubstituted Keggin anion $[\text{PV}_3\text{W}_9\text{O}_{40}]^{6-}$.^[21] Because of the protonation of an external oxygen atom, the central encapsulated PO_4 group is deshielded from $\delta = -12.16$ to

-11.38 . The number of protons on **1** and **2** is dependent on the pH value, and so, for clarity, except when necessary, protons attached to the polyanions are omitted in the following discussion; thus compounds **1** and **2** are denoted as P_4Mo_6 and As_4Mo_6 , respectively.

Arsenate–phosphate exchange in $[\text{H}_7\text{As}_4\text{Mo}_6\text{S}_6\text{O}_{25}]^{5-}$ (2**):** As revealed by variable-temperature ^{31}P NMR experiments, PO_4 groups in **1** are labile. We have examined the exchange of arsenate groups in **2a** for phosphate groups, to build a model for such exchange reactions. Solutions of As_4Mo_6 containing variable amounts of H_2PO_4^- and H_2AsO_4^- ($[\text{HP}]$ and $[\text{HAS}]$, respectively), at a fixed pH value (5.0), were prepared. Three characteristic ^{31}P NMR spectra are shown in Figure 6. Three

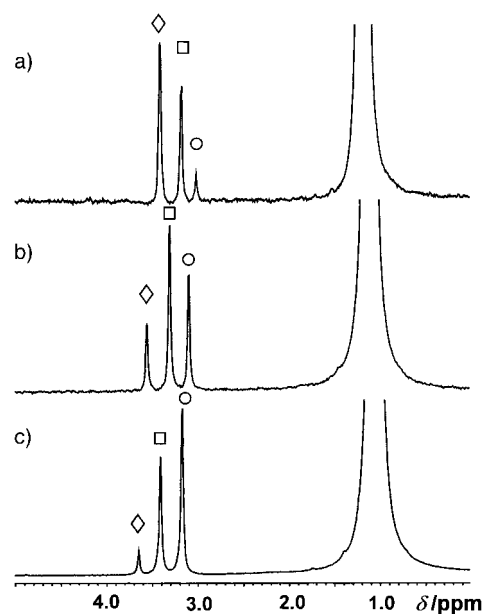


Figure 6. Arsenate–phosphate exchange: ^{31}P NMR spectra of solutions with variable $[\text{P}]/[\text{As}]$ ratios: a) $[\text{P}]/[\text{As}] = 0.33$; b) $[\text{P}]/[\text{As}] = 1.00$; c) $[\text{P}]/[\text{As}] = 4.00$. The three high-frequency peaks have been attributed to As_3PMo_6 (\diamond), $\text{As}_2\text{P}_2\text{Mo}_6$ (\square), and AsP_3Mo_6 (\circ).

resonances are observed at $\delta = +3.43$, $+3.19$, and $+3.03$ for $[\text{HP}]/[\text{HAS}] = 0.33$. The chemical shifts of these three resonances appear to be nearly independent of $[\text{HP}]/[\text{HAS}]$ and are only shifted by $\delta = +0.2$ when $[\text{HP}]/[\text{HAS}]$ increases from 0.33 to 4.00. However, the relative intensities of the three peaks are highly dependent on $[\text{HP}]/[\text{HAS}]$. For low $[\text{HP}]/[\text{HAS}]$ ratios, the $\delta = +3.43$ line is the most intense; its relative intensity decreases as $[\text{HP}]/[\text{HAS}]$ is raised. In concentrated phosphate solutions ($[\text{H}_2\text{PO}_4^-] = 1\text{M}$), the most intense peak is thus observed at $\delta = +3.03$, while two weaker lines are observed at $\delta = +3.43$ and $+3.19$. The chemical shifts of the three resonances are close to that of δ_p , attributed above to the three peripheral phosphate groups. Since no additional line is observed in the range corresponding to the chemical shift of the central phosphate group, the three resonances at $\delta = +3.43$, $+3.19$ and $+3.03$ are definitively attributed to the products resulting from the successive substitutions of

peripheral arsenate groups, namely As_3PMo_6 , $\text{As}_2\text{P}_2\text{Mo}_6$, and AsP_3Mo_6 , according to the simplified Equations (1)–(3).



Determination of As–P exchange constants: The related exchange constants are given by Equations (4)–(6). K_1 , K_2 , and K_3 are apparent constants calculated for a fixed pH value (5.0) and a fixed ionic strength (1M).

$$K_1 = \frac{[\text{As}_3\text{PMo}_6][\text{HAs}]}{[\text{As}_4\text{Mo}_6][\text{HP}]} \quad (4)$$

$$K_2 = \frac{[\text{As}_2\text{P}_2\text{Mo}_6][\text{HAs}]}{[\text{As}_3\text{PMo}_6][\text{HP}]} \quad (5)$$

$$K_3 = \frac{[\text{AsP}_3\text{Mo}_6][\text{HAs}]}{[\text{As}_2\text{P}_2\text{Mo}_6][\text{HP}]} \quad (6)$$

Only the ratios $[\text{As}_2\text{P}_2\text{Mo}_6]/[\text{As}_3\text{PMo}_6]$ (r_2) and $[\text{AsP}_3\text{Mo}_6]/[\text{As}_2\text{P}_2\text{Mo}_6]$ (r_3) can be calculated from ^{31}P NMR integrated intensities since the phosphate-free As_4Mo_6 compound cannot be observed by ^{31}P NMR spectroscopy. The $[\text{HAs}]/[\text{HP}]$ ratios were fixed by the initial conditions chosen for each experiment. The variation of r_2 and r_3 as a function of $[\text{HP}]/[\text{HAs}]$ is linear (Figure 7). The values of K_2 (1.0) and K_3 (0.3) were

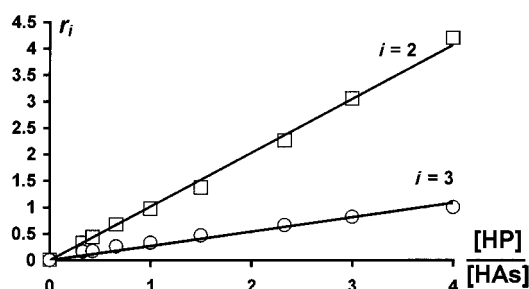


Figure 7. Dependence of r_2 and r_3 (see text) on $[\text{P}]/[\text{As}]$. The slopes of the lines give the As–P exchange constants $K_2 = 1.0$ and $K_3 = 0.3$.

deduced from the slopes of these two lines. A more convenient specific thermodynamic constant, K'_i , can be obtained from the expression for K_i ($i = 1, 2$, or 3) by introducing the concentrations of exchange sites (*As and *P) per anion. K'_i is defined from the formal equilibrium (7).



For the first exchange, represented by Equation (1), the As_4Mo_6 substrate displays three equivalent exchange sites for phosphate ($[\text{*As}] = 3[\text{As}_4\text{Mo}_6]$), whereas in the As_3PMo_6 product only one exchange site is available for arsenate ($[\text{*P}] = [\text{As}_3\text{PMo}_6]$). The corresponding specific constant K'_1 is given by Equation (8). Similarly, the specific constants K'_2 and K'_3 [Eqs. (9) and (10)] are deduced from K_2 and K_3 , respectively [Eqs. (2) and (3)].

$$K'_1 = \frac{[\text{As}_3\text{PMo}_6][\text{HAs}]}{3[\text{As}_4\text{Mo}_6][\text{HP}]} = \frac{K_1}{3} \quad (8)$$

$$K'_2 = K_2 = 1 \quad (9)$$

$$K'_3 = K_3 = 0.9 \quad (10)$$

The closeness of K'_2 and K'_3 indicates that the affinity for the exchange sites involved in Equations (2) and (3) is quite independent of the substitution step; therefore the mean value $K'_i = 1$ can be proposed for the three exchanges; this means that As and P are distributed statistically over the three peripheral sites and the distribution of As_4Mo_6 , As_3PMo_6 , $\text{As}_2\text{P}_2\text{Mo}_6$, and AsP_3Mo_6 depends only on the $[\text{HP}]/[\text{HAs}]$ ratio. Such a result is related to the very similar chemical behavior of arsenate and phosphate (size, charge, and acidity constant).

Phosphate–acetate exchange in $[\text{H}_2\text{P}_4\text{Mo}_6\text{S}_6\text{O}_{25}]^{5-}$ (1): In another set of experiments we studied the exchange of phosphate (P) by acetate (Ac). Acetate was chosen for its good chelating behavior and for its well-adapted $\text{p}K_a$ value (corresponding to the stability domain of H_2PO_4^-). Solutions containing **1a**, variable amounts of acetate buffer (1M CH_3COOH , 1M CH_3COONa) and 1M NaH_2PO_4 were examined at pH 4.65 by ^{31}P NMR spectroscopy. The overall variation in the spectra (Figure 8) was interpreted as resulting

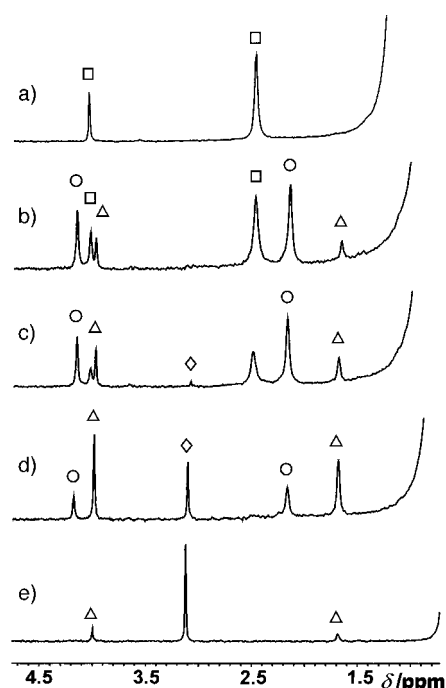


Figure 8. Phosphate–acetate exchange: ^{31}P NMR spectra of solutions containing P_4Mo_6 (\square), P_3AcMo_6 (\circ), $\text{P}_2\text{Ac}_2\text{Mo}_6$ (\triangle), and PAc_3Mo_6 (\diamond) in solutions with variable $[\text{P}]/[\text{HAc}]$ ratios: a) 1M phosphate solution; b) $[\text{P}]/[\text{HAc}] = 4.00$; c) $[\text{P}]/[\text{HAc}] = 2.33$; d) $[\text{P}]/[\text{HAc}] = 0.42$; e) 2M acetate buffer.

from successive exchange reactions leading to mixed acetate–phosphate compounds [Eqs. (11)–(13)].







Compound	$[\text{H}_7\text{P}_4\text{Mo}_6\text{S}_6\text{O}_{25}]^{4-}$	$[\text{H}_6\text{P}_3(\text{CH}_3\text{COO})\text{Mo}_6\text{S}_6\text{O}_{25}]^{3-}$	$[\text{H}_5\text{P}_2(\text{CH}_3\text{COO})_2\text{Mo}_6\text{S}_6\text{O}_{25}]^{2-}$	$[\text{H}_4\text{P}(\text{CH}_3\text{COO})_3\text{Mo}_6\text{S}_6\text{O}_{25}]^{1-}$
Idealized symmetry	P_4Mo_6 (\square) C_{3v}	P_3AcMo_6 (\circ) C_{3v}	$\text{P}_2\text{Ac}_2\text{Mo}_6$ (\triangle) C_{3v}	PAC_3Mo_6 (\diamond) C_{3v}
Polyhedral representation				
δ_c/ppm	+4.35	+4.50	+4.30	+3.40
δ_p/ppm	+2.80	+2.50	+2.00	-

Figure 9. Polyhedral representation of P_4Mo_6 (\square), P_3AcMo_6 (\circ), $\text{P}_2\text{Ac}_2\text{Mo}_6$ (\triangle), and PAC_3Mo_6 (\diamond) with the corresponding ^{31}P NMR chemical shifts of the central and peripheral phosphate groups.

At the same pH (about 4.65) all the compounds are characterized by the resonances of the central phosphate group in the $\delta = 4.5\text{--}3$ range and by the resonances of the peripheral phosphate groups at $\delta < 3$, as already observed for the P_4Mo_6 precursor at the same pH (Figure 5). The relative intensities I_c/I_p corresponding to the central (I_c) and peripheral phosphate groups (I_p) make it possible to characterize unambiguously the compounds resulting from successive substitutions of phosphate by acetate, P_4Mo_6 ($I_c/I_p = 1:3$), P_3AcMo_6 (1:2), $\text{P}_2\text{Ac}_2\text{Mo}_6$ (1:1), and PAC_3Mo_6 (no peripheral phosphate group) (Figures 8 and 9). The proportions of each substituted species were calculated from I_c and I_p at different $[\text{HP}]/[\text{HAc}]$ ratios. From the resulting distribution of the different species in solution (Figure 10), the apparent constants at pH 4.65 were calculated: $K_1 = 5.85$ [Eq. (11)], $K_2 = 1.25$ [Eq. (12)], and $K_3 = 0.20$ [Eq. (13)]. The very good agreement between calculated and experimental distributions confirms the proposed exchange scheme.

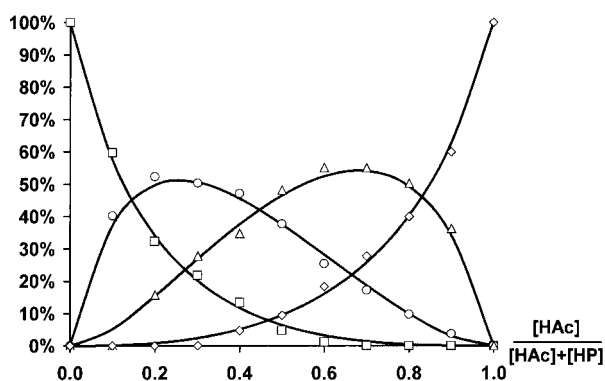


Figure 10. Phosphate-acetate exchange: experimental (points) and calculated (solid lines) species distribution diagram as a function of the ratio $[\text{HAc}]/([\text{P}] + [\text{HAc}])$.

Conclusion

Two new mixed oxo-thio $[\text{H}_7\text{X}_4\text{Mo}_6\text{S}_6\text{O}_{25}]^{5-}$ ($\text{X} = \text{P}, \text{As}$) ions have been synthesized and fully characterized in aqueous solution and by solid-state structure determinations. In

solution, ^{31}P NMR spectroscopy has provided evidence that the peripheral groups can be easily substituted; these results illustrate the value of stereospecific substitution as a method to prepare new functionalized polyanions. Preliminary experiments confirm that reactions similar to those discussed here, with dicarboxylate and diphosphonate in place of acetate and phosphate, can be developed. Such bifunctional ligands could induce multidimensional arrangements with covalently linked $\{\text{X}_4\text{Mo}_6\text{S}_6\text{O}_{25}\}$ building units. It is well known that the condensation, under hydrothermal conditions, of the exclusively oxo precursor $[\text{Mo}_2\text{O}_4]^{2+}$ gives solids that are structural analogues of the thio compounds described here. These two approaches merit being linked by a study of the condensation, under mild conditions, of the preformed $[\text{Mo}_2\text{O}_4]^{2+}$ cation, accompanied by a comparison of the possibilities of exchange properties, which would highlight the role of sulfur in these acid-base reactions as well as in the reactivity of the polyanions.

Experimental Section

$\text{Na}_4\text{Cs}_4\text{Cl}_2[\text{H}_6\text{P}_4\text{Mo}_6\text{S}_6\text{O}_{25}] \cdot 13\text{H}_2\text{O}$ (1a): $\text{K}_{2.6}(\text{NMe}_4)_{0.4}\text{I}_{0.3}[\text{Mo}_{12}\text{S}_{12}\text{O}_{12}(\text{OH})_{12}(\text{H}_2\text{O})_6] \cdot 30\text{H}_2\text{O}$ ^{14,51} (1 g, 0.33 mmol) was dissolved in HCl solution (10 mL, 4 M) and heated for 10 min at 50 °C for complete hydrolysis. Then $\text{NaH}_2\text{PO}_4 \cdot 2\text{H}_2\text{O}$ (1.6 g, 10 mmol) was added to the solution and the pH was adjusted to 5.0 by dropwise addition of a solution of NaOH (4 M). ^{31}P NMR measurements confirmed that $[\text{H}_6\text{P}_4\text{Mo}_6\text{S}_6\text{O}_{25}]^{6-}$ was formed rapidly and represented the only phosphate-containing species in the solution. Addition of cesium chloride (1.5 g; 9 mmol) gave a red-orange precipitate (1.4 g; 95% based on Mo), which was collected by filtration, washed with EtOH, and dried with Et_2O . IR (KBr pellets): $\tilde{\nu} = 1155$ (m), 1129 (m), 1065 (s), 1019 (s), 934 (w), 911 (m), 873 (s), 656 (w), 594 (m), 546 (w), 505 (m), 451 (w), 343 (w) cm^{-1} . $\text{H}_{32}\text{Cl}_2\text{Cs}_4\text{Mo}_6\text{Na}_4\text{O}_{38}\text{P}_4\text{S}_6$: calcd. Cl 3.26, Cs 24.48, Mo 26.50 Na 4.23, P 5.70, S 8.80; found Cl 3.07, Cs 25.00, Mo 26.29, Na 4.44, P 6.30, S 8.30. The number of water molecules was checked by thermogravimetric analysis (Perkin-Elmer TGA 7 Analyzer).

$\text{Na}_{1.75}\text{Rb}_4\text{Cl}_{0.75}[\text{H}_7\text{P}_4\text{Mo}_6\text{S}_6\text{O}_{25}] \cdot 8\text{H}_2\text{O}$ (1b): The synthesis procedure was similar to that for **1a** except that the pH of the solution was adjusted to 4.0 instead of 5.0. After addition of rubidium chloride (1.0 g, 8 mmol) the solution was filtered and the filtrate was allowed to stand at room temperature for crystallization. Red well-shaped hexagonal crystals, suitable for X-ray structure determinations, were collected after several days. $\text{H}_{23}\text{Cl}_{0.75}\text{Mo}_6\text{Na}_{1.75}\text{O}_{33}\text{P}_4\text{Rb}_4\text{S}_6$: calcd. Cl 1.43, Mo 31.10, Na 2.17, P 6.69, Rb 18.46, S 10.39, found Cl 1.62, Mo 30.35, Na 1.86, P 6.70, Rb 18.68, S 10.18.

Na_{1.5}Cs₄Cl_{0.5}[H₇As₄Mo₆S₆O₂₅·13H₂O (2a): K_{2.6}(NMe₄)_{0.4}I₃[Mo₁₂S₁₂O₁₂-(OH)₁₂(H₂O)₆]₃·30H₂O^[4, 5] (1 g, 0.33 mmol) was dissolved in HCl (10 mL, 4 M) and heated for 10 min at 50 °C for hydrolysis. A concentrated solution of H₃AsO₄ (1.0 mL, 11 mmol) was added; the resulting solution was filtered and the pH was adjusted to 4.0 by addition of NaOH (4 M). After addition of cesium chloride (1.5 g, 9 mmol), the red-orange solid (1.4 g, 92% based on Mo) formed was collected by filtration, washed with EtOH and dried with Et₂O. IR (KBr pellets): $\tilde{\nu}$ = 933 (s), 874 (w), 834 (s), 745 (m), 485 (s), 440 (w) cm⁻¹. H₃₃As₄Cl_{0.5}Cs₄Mo₆Na_{1.5}O₃₈S₆: calcd. As 13.04, Cl 0.77, Cs 23.13, Mo 25.04, Na 1.50, S 8.34; found As 12.68, Cl 0.61, Cs 22.50, Mo 25.70, Na 1.40, S 8.36. The number of water molecules was checked by TGA.

Rb_{3.5}Na_{1.5}[H₇As₄Mo₆S₆O₂₅·13H₂O (2b): The synthesis procedure was similar to that of **2a** up to the precipitation step. Solid rubidium chloride (1.0 g, 8 mmol) was added instead of cesium chloride. The solution was filtered and the resulting filtrate was allowed to stand at room temperature for crystallization. Red crystals of **2b**, suitable for a complete X-ray diffraction study, were collected after several days. H₃₃As₄Mo₆Na_{1.5}O₃₈Rb_{3.5}S₆: calcd. As 14.67, Mo 28.19, Na 1.69, Rb 14.65, S 9.40; found As 14.15, Mo 28.40, Na 1.37, Rb 15.68, S 8.73. The number of water molecules was checked by TGA.

Spectroscopy: Infrared spectra were recorded on an IRFT Magna 550 Nicolet spectrophotometer at 0.5 cm⁻¹ resolution, using the technique of pressed KBr pellets.

³¹P NMR spectra were recorded on a Bruker AC-300 spectrometer operating at 121.5 MHz with 5 mm tubes. ³¹P chemical shifts were referenced to the usual external standard, H₃PO₄ (85%). The pH dependence of chemical shifts was studied at room temperature on solutions containing phosphate buffer (1 M) and **1a** (10⁻² M). The arsenate-phosphate exchange was studied on samples containing H₂XO₄⁻ 1 M (X = As, P) and **2a** (10⁻² M). Phosphate-acetate exchange was studied on samples **1a** (10⁻² M) containing variable ratios of acetate buffer (2 M; pH 4.65) and NaH₂PO₄ (1 M) solution.

Crystallography: Compound **2b** rapidly loses water of crystallization, leading to an amorphous solid. Single crystals of **2b** were therefore mounted in Lindeman tubes (0.3 mm diameter). Intensity data for **1b** and **2b** were collected at room temperature (293 K) with a Siemens SMART three-circle diffractometer equipped with a CCD bidimensional detector using MoK α monochromatized radiation (λ = 0.71073 Å). An empirical absorption correction was applied (SADABS program^[18] based on Blessing's method^[19]). The structures were solved by direct methods and refined by full-matrix least-squares procedures (SHELX-TL package^[20]).

Crystallographic data are reported in Table 1 and selected bond lengths in Table 2. Some of the alkali metal cations in **1b** and **2b** and Cl2 in **1b** were found to be disordered. The occupancy factors of these atoms were refined and then set to 1/2 (Na2 in **1b**), 1/4 (Rb3A and Rb3B in **2b**), 1/2 (Na2 in **2b**), and 1/2 (Cl2 in **1b**). A rubidium cation was missing in **2b**, probably because of a large disorder in the range of counterions and water molecules, as is often observed for structures of such compounds.^[21] For this reason, the exact formula was determined by elemental analysis. All the disordered atoms and the water molecules in **2b** were refined isotropically, the other atoms anisotropically. The residual electron density (2.99 e Å⁻³ for **1b** and 3.74 e Å⁻³ for **2b**) is located in the vicinity of the disordered alkali cations. Further details of the crystal structure investigations can be obtained from the Fachinformationszentrum Karlsruhe, D-76344 Eggenstein-Leopoldshafen (Germany) (fax: (+49) 7247-808-666; e-mail: crysdata@fiz.karlsruhe.de) on quoting the depository numbers CSD-410688 for **1b** and CSD-410687 for **2b**.

Table 1. Crystallographic data for **1b** and **2b**.

	1b	2b
formula	H ₁₉ Cl _{0.75} Mo ₆ Na _{1.75} O ₃₁ P ₄ Rb ₄ S ₆	H ₃₃ As ₄ Mo ₆ Na _{1.5} O ₃₈ Rb _{3.5} S ₆
<i>M_r</i>	1815.7	2042.6
crystal size [mm]	0.05 × 0.26 × 0.36	0.24 × 0.30 × 0.60
crystal system	rhombohedral	triclinic
space group	<i>R</i> $\bar{3}$	<i>P</i> $\bar{1}$
<i>a</i> [Å]	13.352(3)	12.967(1)
<i>b</i> [Å]	13.352(3)	13.271(1)
<i>c</i> [Å]	39.708(10)	15.870(1)
α [°]	90	101.11(1)
β [°]	90	91.81(1)
γ [°]	120	115.94(1)
<i>V</i> [Å ³]	6131(2)	2389(1)
<i>Z</i>	6	2
ρ_{calc} [g cm ⁻³]	2.951	2.840
μ [mm ⁻¹]	7.141	8.192
θ range [°]	1.83–29.77	1.32–29.73
reflections measured	6211	16243
unique reflections (<i>R</i> _{int})	3486 (0.044)	11573 (0.055)
observed (<i>I</i> > 2 σ (<i>I</i>))	2803	7169
refined parameters	171	462
<i>R</i> ₁ (<i>F</i>) ^[a]	0.055	0.069
<i>wR</i> ₂ (<i>F</i> ²) ^[b]	0.144	0.188

[a] $R_1 = \sum |F_o| - |F_c| / \sum |F_o|$. [b] $wR_2 = (\sum w(F_o^2 - F_c^2)^2 / \sum w(F_o^2)^2)^{0.5}$ with $w = 1 / (\sigma^2 F_o^2 + (aP)^2 + bP)$, where $P = (F_o^2 + 2F_c^2) / 3$, and $a = 0.0717$, $b = 204.33$ for **1b**; $a = 0.100$, $b = 0$ for **2b**.

Table 2. Selected bond lengths [Å] in **1b** and **2b**.

1b			
Mo1–O1	1.697(6)	Mo2–O2	1.695(6)
Mo1–O5	2.111(5)	Mo2–O3	2.094(6)
Mo1–O4	2.115(7)	Mo2–O5	2.115(5)
Mo1–S2	2.308(2)	Mo2–S2	2.308(2)
Mo1–S1	2.317(2)	Mo2–S1	2.317(2)
Mo1–O6	2.335(6)	Mo2–O6	2.333(6)
Mo1–Mo2	2.8232(11)		
P1–O7	1.508(10)	P2–O4	1.502(7)
P1–O6	1.553(5)	P2–O3	1.530(6)
P2–O9	1.498(8)	P2–O8	1.583(8)
2b			
Mo1A–O1A	1.689(9)	Mo1C–O4B	2.136(8)
Mo1A–O4C	2.132(7)	Mo1C–S1C	2.322(3)
Mo1A–O5C	2.132(7)	Mo1C–S2C	2.323(3)
Mo1A–S2A	2.315(3)	Mo1C–O6B	2.385(7)
Mo1A–S1A	2.321(3)	Mo1C–Mo2C	2.8383(13)
Mo1A–O6C	2.382(7)	Mo2C–O2C	1.670(7)
Mo1A–Mo2A	2.8351(12)	Mo2C–O3C	2.117(7)
Mo2A–O2A	1.691(9)	Mo2C–O5C	2.120(8)
Mo2A–O5A	2.127(7)	Mo2C–S2C	2.317(3)
Mo2A–O3A	2.127(8)	Mo2C–S1C	2.322(3)
Mo2A–S2A	2.321(3)	Mo2C–O6C	2.373(7)
Mo2A–S1A	2.327(3)	As1–O6B	1.675(7)
Mo2A–O6A	2.335(7)	As1–O6A	1.679(7)
Mo1B–O1B	1.681(8)	As1–O6C	1.690(6)
Mo1B–O4A	2.133(8)	As1–O7	1.720(7)
Mo1B–O5A	2.153(8)	As2A–O4A	1.661(9)
Mo1B–S1B	2.311(3)	As2A–O8A	1.675(8)
Mo1B–S2B	2.319(3)	As2A–O3A	1.693(8)
Mo1B–O6A	2.382(7)	As2A–O9A	1.728(8)
Mo1B–Mo2B	2.8441(14)	As2B–O8B	1.654(8)
Mo2B–O2B	1.699(8)	As2B–O3B	1.652(7)
Mo2B–O3B	2.109(8)	As2B–O4B	1.680(8)
Mo2B–O5B	2.119(7)	As2B–O9B	1.729(9)
Mo2B–S1B	2.313(3)	As2C–O8C	1.666(8)
Mo2B–S2B	2.318(3)	As2C–O3C	1.678(8)
Mo2B–O6B	2.401(7)	As2C–O4C	1.684(7)
Mo1C–O1C	1.680(8)	As2C–O9C	1.734(8)
Mo1C–O5B	2.115(7)		

[1] A. Müller, E. Dieman, *Adv. Inorg. Chem. Radiochem.* **1987**, *31*, 89.[2] a) E. Cadot, V. Béreau, B. Marg, S. Halut, F. Sécheresse, *Inorg. Chim. Acta* **1996**, *25*, 3099; b) E. Cadot, V. Béreau, F. Sécheresse, *Inorg. Chim. Acta* **1996**, *252*, 101.[3] a) F. Sécheresse, E. Cadot, V. Béreau, *Recent Progress in Polyoxometalate Chemistry*, Paris, November 21–23, **1996**; b) V. Béreau, E. Cadot, F. Sécheresse, A. Müller, H. Bögge, E. Krickemeyer, *Inorg. Chem.* submitted.[4] E. Cadot, B. Salignac, S. Halut, F. Sécheresse, *Angew. Chem.* **1998**, *110*, 631; *Angew. Chem. Int. Ed. Engl.* **1998**, *37*, 612.

- [5] A. Dolbecq, E. Cadot, F. Sécheresse, *J. Chem. Soc. Chem. Commun.* **1998**, 2293.
- [6] For a review, see: R. C. Haushalter, L. A. Mundi, *Chem. Mater.* **1992**, *4*, 31.
- [7] C. G. Kim, D. Coucouvanis, *Inorg. Chem.* **1993**, *32*, 2232.
- [8] G. A. Zank, T. B. Rauchfuss, S. R. Wilson, *J. Am. Chem. Soc.* **1984**, *106*, 7621.
- [9] J.-H. Chou, J. A. Hanco, M. G. Kanatzidis, *Inorg. Chem.* **1997**, *36*, 4.
- [10] R. J. Francis, D. O'Hare, *J. Chem. Soc. Dalton Trans.* **1998**, 3133.
- [11] E. Cadot, B. Salignac, T. Loiseau, F. Sécheresse, *Chem. Eur. J.* **1999**, in press.
- [12] a) R. C. Haushalter, F. W. Lai, *Angew. Chem.* **1989**, *101*, 802; *Angew. Chem. Int. Ed. Engl.* **1989**, *28*, 743; b) R. C. Haushalter, F. W. Lai, *Inorg. Chem.* **1989**, *28*, 2905; c) L. A. Mundi, R. C. Haushalter, *Inorg. Chem.* **1992**, *31*, 3050; d) L. Meyer, R. C. Haushalter, *Inorg. Chem.* **1993**, *32*, 1579.
- [13] a) P. Lightfoot, D. Masson, *Mater. Res. Bull.* **1995**, *30*, 1005; b) P. Lightfoot, D. Masson, *Acta Crystallogr. Sect. C* **1996**, *52*, 1077.
- [14] a) A. Guesdon, M. M. Borel, A. Leclaire, B. Raveau, *Chem. Eur. J.* **1997**, *3*, 1797; b) A. Leclaire, C. Biot, H. Rebbah, M. M. Borel, B. Raveau, *J. Mater. Chem.* **1998**, *8*, 439.
- [15] M. I. Khan, Q. Chen, J. Zubieta, *Inorg. Chim. Acta* **1995**, 235, 135.
- [16] A. Dolbecq, B. Salignac, E. Cadot, F. Sécheresse, *Bull. Pol. Acad. Sci.* **1998**, *46*, 237.
- [17] P. J. Domaille, G. Watanuya, *Inorg. Chem.* **1986**, *25*, 1239.
- [18] G. M. Sheldrick, SADABS: Program for Scaling and Correction of Area Detector Data, University of Göttingen (Germany), **1997**.
- [19] R. Blessing, *Acta Crystallogr. Sect. A* **1995**, *51*, 33.
- [20] G. M. Sheldrick, SHELX-TL version 5.03, Software Package for Crystal Structure Determination, Siemens Analytical X-ray Instrument Division, Madison (WI), **1994**.
- [21] a) F. Xiu, M. T. Pope, *Organometallics* **1994**, *13*, 4881; b) M. Bösing, I. Loose, H. Pohlmann, B. Krebs, *Chem. Eur. J.* **1997**, *3*, 1232.

Received: February 1, 1999 [F1580]